

# Modeling and Simulation of Dynamics of Differential Gear Train Mechanism using Bond Graph

Saurabh Goyal

Mechanical Department  
Dr. B. R. Ambedkar NIT, Jalandhar  
Jalandhar, India  
saurabhgoyal150989@gmail.com

Anand Vaz

Mechanical Department  
Dr. B. R. Ambedkar NIT, Jalandhar  
Jalandhar, India  
anandvaz@ieee.org

**Abstract** - In this paper, dynamics of the well-known differential gear train mechanism is presented in a systematic manner using the unified approach of bond graph. The approach offers an alternative to the conventional energy based methods. The dynamics of the mechanism is also quite significant from the point of view of design. Reaction forces and moments at different locations, which are of interest from the design perspective, have been presented. Rigid body dynamics is applied to model each link of the mechanism. The links are constrained suitably based on the nature of interaction between consecutive links. In this work, the code for simulation is directly written from the bond graph, without formally deriving system equations. Simulation results provide insight into the dynamics of the differential mechanism.

**Keywords** - Bond Graph, Modeling, Simulation, Differential gear train, Rigid body dynamics

## I. INTRODUCTION

Bond graph [1, 2], are graphical tools which can be used to model and analyse the dynamic behaviour of various multi-energy systems. In addition, cause and effect relationship between the subsystems are conveniently represented. The notion of causality, apart from aiding with the formulation of system equations which govern the behaviour of the system, help in pointing out any physical impossibility or system property we may have failed to take into account in the modeling stage [1, 2]. Simulation has become an indispensable analytical tool using which one can experiment with a system at little or no expense. In this work, a multibond graph (MBG) approach is used to model the dynamics of the differential gear train mechanism [3]. Using this Bond Graph model, we simulate the dynamic behaviour of the mechanism. This establishes a very effective method of predicting the behaviour of systems, which, in a number of applications, can prove to be economical as well as time saving. In general, mechanical systems can be treated as a finite number of rigid bodies which are constrained suitably based on the nature of interaction between consecutive links. Kinematics of such mechanisms is usually available in most texts and reference books on machines and mechanisms [3, 4]. However, the dynamics is rarely presented although it is extremely important from the design perspective. Using the Bond Graph approach, simulation can be conveniently carried out in MATLAB [5], and the dynamic quantities like reaction forces and moments at various locations on the system can be determined, plotted and analysed.

The idea of modeling the differential mechanism using bond graph was presented in 1992 by Karnopp [6]. Only the rotational dynamics was considered and an issue of derivative causality arising in mechanism models was addressed. The planet gears of the differential mechanism not only have rotational but translational motion as well. Consequently centrifugal forces on planets arise and have to be borne by appropriate reactions at the bearings on the crown arms. This aspect was not taken into account in Karnopp's work. The model presented in this work is capable of handling rotational as well as translational dynamics arising in the differential mechanism.

This paper is organized as follows. The next section describes the construction of the bond graph model for the differential mechanism. Simulation results for the various links have been presented and discussed in section 3, followed by conclusions.

## II. MODELING

In this section, we develop a multi-bond graph model of the differential gear train mechanism, representing the translation and rotation for each rigid link of the system. The differential gear train mechanism is used to transmit power from the engine-gear box system to the rear wheels of automobiles, and to rotate the rear wheels at different speeds while the automobile is taking a turn. The differential gear train mechanism consists of a number of rigid bodies (links) as shown in Fig. 1. Rigid body dynamics [7], is applied to model each link. The links are constrained suitably based on the nature of interaction between consecutive links. Modeling of rigid body dynamics using multibond graph was presented by Tiernego and Bos in 1985 [8]. Vaz and Hirai [9] had presented the application of multibond graph to the modeling of spatial dynamics of prosthetic devices in 2004. Rotational motion was expressed in the inertial frame, leading to the elimination of the Euler junction structure. The resulting model is computationally more economical even though the inertia tensor changes with change in orientation [10].

Seven rigid moving links of the differential gear train have been identified as: link  $G$  – gear on the propeller shaft, link  $A$  – crown wheel, links  $P1$  and  $P2$  – two planet gears, links  $S1$  and  $S2$  – two sun gears and link  $H$  – the housing which covers all these rigid links. The links have relative motion with respect to each other and also with respect to a stationary frame  $O$ . The housing is also assumed to be fixed with respect to the inertial

frame. Each of these rigid links is modeled using multibond graphs (MBG).

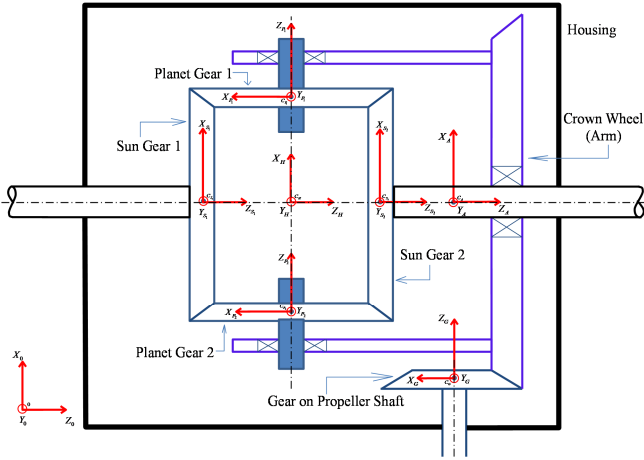


Fig. 1. Differential Gear Train Mechanism

For modeling of each link we fix the frame on each link by using the Denavit – Hartenberg convention [11], commonly known as D-H convention. Frame  $H$  is fixed on the link  $H$  (housing), frame  $G$  is fixed on the link  $G$  (gear on the propeller shaft), frame  $A$  is fixed on the link  $A$  (crown wheel), frames  $P1$  and  $P2$  are fixed on the links  $P1$  and  $P2$  (Planet gears) and frames  $S1$  and  $S2$  are fixed on the links  $S1$  and  $S2$  (sun gears). Also,  $C_H, C_G, C_A, C_{P1}, C_{P2}, C_{S1}$  and  $C_{S2}$  are the centers of mass of the respective links as shown in Fig. 1. The translational effect of each link is concentrated at its center of mass, while the rotational effect is considered in the inertial frame itself by considering the inertia tensor for each link about its respective center of mass and expressed in the inertial frame.

The Bond graph modeling is initiated with the representation of kinematic relationships.  $\mathbf{1}_{0\bar{\omega}_G}$  Junction represents the angular velocity of the gear  $G$  on propeller shaft. Similarly, the angular velocities of the crown wheel  $A$ , housing  $H$ , planet gears  $P1$  and  $P2$ , sun gears  $S1$  and  $S2$ , are represented using  $\mathbf{1}_{0\bar{\omega}_A}, \mathbf{1}_{0\bar{\omega}_H}, \mathbf{1}_{0\bar{\omega}_{P1}}, \mathbf{1}_{0\bar{\omega}_{P2}}, \mathbf{1}_{0\bar{\omega}_{S1}}, \mathbf{1}_{0\bar{\omega}_{S2}}$  junctions. We take  ${}^H_0\bar{\omega}_G$  as relative angular velocity of  $\mathbf{1}_{0\bar{\omega}_G}$  junction with respect to  $\mathbf{1}_{0\bar{\omega}_H}$  junction. Similarly,  ${}^H_0\bar{\omega}_A$  as relative angular velocity of  $\mathbf{1}_{0\bar{\omega}_A}$  junction with respect to  $\mathbf{1}_{0\bar{\omega}_H}$  junction and similarly  ${}^A_0\bar{\omega}_{P1}, {}^A_0\bar{\omega}_{P2}, {}^A_0\bar{\omega}_{S1}$  and  ${}^A_0\bar{\omega}_{S2}$  are the relative angular velocities for junctions  $\mathbf{1}_{0\bar{\omega}_{P1}}, \mathbf{1}_{0\bar{\omega}_{P2}}, \mathbf{1}_{0\bar{\omega}_{S1}}$ , and  $\mathbf{1}_{0\bar{\omega}_{S2}}$  with respect to  $\mathbf{1}_{0\bar{\omega}_A}$  junction. After that we observe the relative motion of gear on propeller shaft and crown wheel with respect to the housing and express these in the frame of housing itself by using a modulated transformer  $\mathbf{MTF}: {}^H_0R$ . Similarly, we observe the relative motion of planet gears and sun gears with respect to the crown wheel and express in the frame of crown wheel itself by using a modulated transformer  $\mathbf{MTF}: {}^A_0R$ . Thus, we establish a gear ratio relationship between motion of the gear on propeller shaft

and crown wheel and between planet gears and sun gears by using a transformer (TF). Further constraints are applied on the links (gear on the propeller shaft, crown wheel, planet gears and sun gears) in the proper directions depending on the frame they are going to be observed and expressed in. Likewise,  $\mathbf{1}_{0\dot{r}_{CG}}$

junction represents the translational velocity of the gear  $G$  on propeller shaft. Similarly, the translational velocities of the crown wheel  $A$ , housing  $H$ , planet gears  $P1$  and  $P2$ , sun gears  $S1$  and  $S2$ , are represented using  $\mathbf{1}_{0\dot{r}_{CA}}, \mathbf{1}_{0\dot{r}_{CH}}, \mathbf{1}_{0\dot{r}_{CP1}}, \mathbf{1}_{0\dot{r}_{CP2}}, \mathbf{1}_{0\dot{r}_{CS1}}, \mathbf{1}_{0\dot{r}_{CS2}}$  junctions. By using the relations

$${}^0\dot{r}_{CG} = {}^0\dot{r}_{CH} + [{}^0C_G\bar{r}_{CH} \times] {}^0\bar{\omega}_H, \quad (1)$$

$${}^0\dot{r}_{CA} = {}^0\dot{r}_{CH} + [{}^0C_A\bar{r}_{CH} \times] {}^0\bar{\omega}_H, \quad (2)$$

we described the relative translational velocity between  $\mathbf{1}_{0\dot{r}_{CG}}$  and  $\mathbf{1}_{0\dot{r}_{CH}}$  junction and between  $\mathbf{1}_{0\dot{r}_{CA}}$  and  $\mathbf{1}_{0\dot{r}_{CH}}$  junction. Similarly,

$${}^0\dot{r}_{CP1} = {}^0\dot{r}_{CA} - [{}^0C_A\bar{r}_{CP1} \times] {}^0\bar{\omega}_A, \quad (3)$$

$${}^0\dot{r}_{CP2} = {}^0\dot{r}_{CA} - [{}^0C_A\bar{r}_{CP2} \times] {}^0\bar{\omega}_A, \quad (4)$$

we described the relative translational velocity between  $\mathbf{1}_{0\dot{r}_{CP1}}$  and  $\mathbf{1}_{0\dot{r}_{CA}}$  junction and between  $\mathbf{1}_{0\dot{r}_{CP2}}$  and  $\mathbf{1}_{0\dot{r}_{CA}}$  junction.

$${}^0\dot{r}_{CS1} = {}^0\dot{r}_{CH} + [{}^0C_{S1}\bar{r}_{CH} \times] {}^0\bar{\omega}_H, \quad (5)$$

$${}^0\dot{r}_{CS2} = {}^0\dot{r}_{CH} + [{}^0C_{S2}\bar{r}_{CH} \times] {}^0\bar{\omega}_H, \quad (6)$$

we described the relative translational velocity between  $\mathbf{1}_{0\dot{r}_{CS1}}$  and  $\mathbf{1}_{0\dot{r}_{CH}}$  junction and between  $\mathbf{1}_{0\dot{r}_{CS2}}$  and  $\mathbf{1}_{0\dot{r}_{CH}}$  junction respectively.

After specifying kinematic relationships between all the links, cause and effect relationships between the subsystems are assigned. The notion of causality, apart from aiding with the formulation of the system equations which govern the behaviour of the system, help in pointing out any physical impossibility or system property that had been missed out at the modeling stage. While modeling the differential gear train mechanism, derivative causality arises, and is rectified by introduction of suitable viscoelastic subsystems given by  $\mathbf{C}$  and  $\mathbf{R}$  elements. The resulting bond graph becomes integrally causalem. The code for simulation is directly written from the bond graph model by tracing causal paths, even without explicitly deriving the system equations. One can also derive system equations explicitly, from the bond graph, for the purpose of analysis.

In this work, the link  $H$  (housing) is fixed by applying a source of flow  $S_F = \bar{0}$  on the angular velocity of the housing

and also on the translational velocity of the housing, so that the motion of housing, as observed and expressed in the inertial

frame, is constrained. The dynamics of the system of Fig. 1 is modeled in the multibond graph shown in Fig. 2.

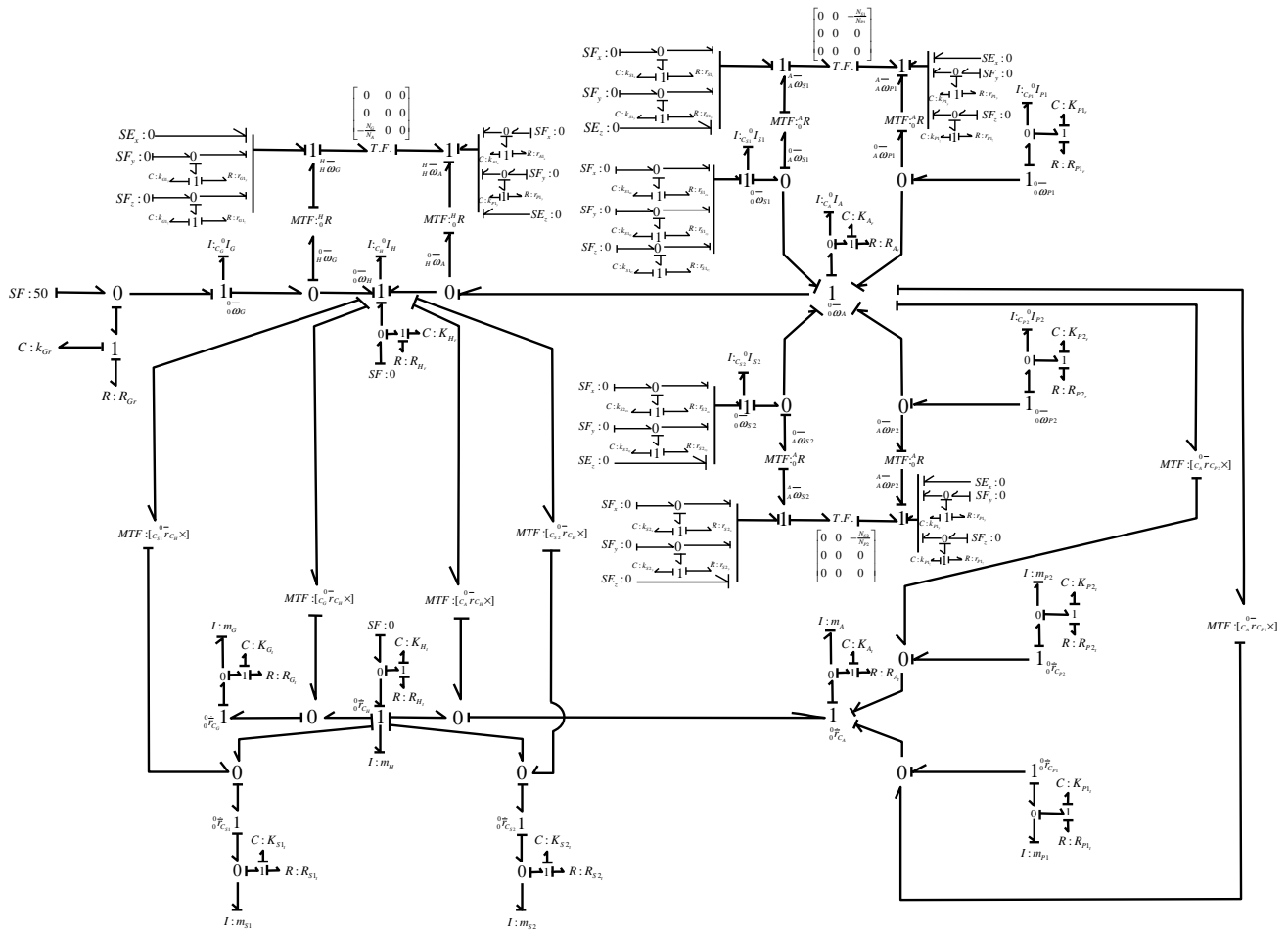


Fig. 2. Multibond graph model of Differential gear train mechanism

### III. SIMULATION OF THE DIFFERENTIAL MECHANISM

The Bond Graph model has been simulated using MATLAB. Simulation results are shown in this section. For simulation, source of flow of 50 rad/sec is applied on link *G*. This causes the crown wheel (link *A*) to rotate. We constrain the motion of one of the sun gears. Sun gear 2 (Link *S2*) is free to rotate. Various simulation results have been obtained. Table 1 shows the values of the various link parameters used in the simulation, whereas table 2 shows the values of the stiffness and damping of the various couplings used.

TABLE I. LINK PARAMETERS

	Density	Diameter	No. of Teeth	Thickness
Gear	2700 Kg/m <sup>3</sup>	0.1 m	12	0.01 m
Crown Wheel (Arm)	2700 Kg/m <sup>3</sup>	0.4 m	48	0.01 m
Planet Gears (1, 2)	2700 Kg/m <sup>3</sup>	0.1 m	12	0.01 m
Sun Gears (1, 2)	2700 Kg/m <sup>3</sup>	0.2 m	24	0.01 m

TABLE II. VALUES OF STIFFNESS AND DAMPING OF DIFFERENT COUPLINGS USED FOR SIMULATION

	Stiffness	Damping
Rotational coupling between source of zero angular velocity and housing	$K = 1000000 \text{ N.m/rad}_{Hr}$	$R = 20 \text{ N.m.s/rad}_{Hr}$
Translational coupling between source of zero linear velocity and housing	$K = 1000000 \text{ N/m}_{Hr}$	$R = 20 \text{ N.s/m}_{Hr}$
Rotational coupling between source of constant angular velocity and gear on propeller shaft	$K = 1000 \text{ N.m/rad}_{Gr}$	$R = 5 \text{ N.m.s/rad}_{Gr}$
Translational coupling parameters for gear on propeller shaft	$K = 1000000 \text{ N/m}_{Gr}$	$R = 20 \text{ N.s/m}_{Gr}$
Rotational coupling parameters for crown wheel	$K = 1000 \text{ N.m/rad}_{Ar}$	$R = 2 \text{ N.m.s/rad}_{Ar}$
Translational coupling parameters for crown wheel	$K = 1000000 \text{ N/m}_{At}$	$R = 20 \text{ N.s/m}_{At}$
Rotational coupling parameters for planet gear 1, 2	$K = K_{P1r} = K_{P2r} = 1000 \text{ N.m/rad}$	$R = R_{P1r} = R_{P2r} = 0.1 \text{ N.m.s/rad}$
Translational coupling	$K = K_{P1t} = K_{P2t} = 1000000$	$R = R_{P1t} = R_{P2t} = 20$

parameters for planet gear 1, 2	N/m	N.s/m
Translational coupling parameters for sun gear 1, 2	$K_{S1t} = K_{S2t} = 1000000$ N/m	$R_{S1t} = R_{S2t} = 20$ N.s/m
Rotational coupling between gear on propeller shaft and housing	$K_{Gly} = K_{Glz} = 10000$ N.m/rad	$R_{Gly} = R_{Glz} = 10$ N.m.s/rad
Rotational coupling between crown wheel and housing	$K_{Alx} = K_{Aly} = 1000$ N.m/rad	$R_{Alx} = R_{Aly} = 10$ N.m.s/rad
Rotational coupling between planet gears and crown wheel	$K_{Ply} = K_{Plz} = K_{P2y} = K_{P2z} = 1000$ N.m/rad	$R_{Ply} = R_{Plz} = R_{P2y} = R_{P2z} = 10$ N.m.s/rad
Rotational coupling between sun gears and crown wheel	$K_{S1x} = K_{S1y} = K_{S2x} = K_{S2y} = 1000$ N.m/rad	$R_{S1x} = R_{S1y} = R_{S2x} = R_{S2y} = 10$ N.m.s/rad
Rotational coupling between source of zero angular velocity and sun gear1	$K_{S1rx} = K_{S1ry} = K_{S1rz} = 100000$ N.m/rad	$R_{S1rx} = R_{S1ry} = R_{S1rz} = 5$ N.m.s/rad
Rotational coupling between source of zero angular velocity and sun gear2	$K_{S2rx} = K_{S2ry} = 100000$ N.m/rad	$R_{S2rx} = R_{S2ry} = 5$ N.m.s/rad

### Simulation Plots:

The simulation plots for the different links have been discussed in the following sections.

#### A. Link G (Gear)

As the link G starts rotating from its initial position, the orientation of the link G continuously changes with time. The columns of the orientation matrix  ${}^0_G R$  represent the motion of tip of the unit vectors with respect to a stationary frame 0. The tip of unit vector in x and y direction moves in a circle as the link G rotates in the y-z plane about x axis as seen from the inertial frame. And tip of the unit vector in z direction is seen as a point because unit vector in z direction does not change its orientation. Fig. 3 shows all the three columns of orientation matrix of link G.

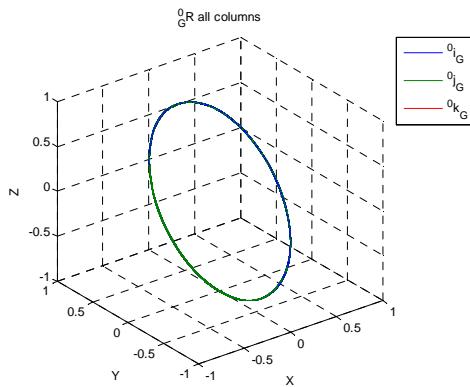


Fig. 3. Orientation matrix of link G  ${}^0_G R$

Fig. 4 shows the variation of components of the position vector  ${}^0_{0} \vec{r}_{C_G}$  of the center of the mass of the link G with time which is constant because center of mass of link G does not change its position with respect to time. Hence, center of mass of link G does not trace any path.

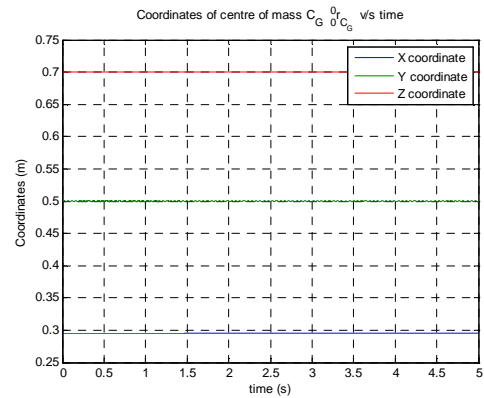


Fig. 4. Variation of coordinates of center of mass of link G with time

Fig. 5 indicates the variation in the angular momentum of the link G as it rotates. The angular momentum vector has only the x component as the rotation is about the x axis. As indicated in the fig. 5, the angular momentum first increase and then almost constant with time. This is due to the constant value of source of flow  $S_f$  imposed on the link G in the x direction as observed and expressed in the inertial frame.

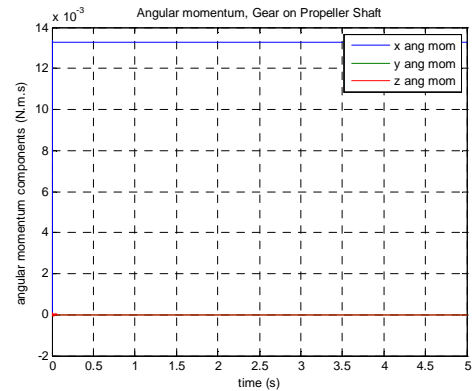


Fig. 5. Variation of components of momentum of link G with time

We have considered a constant source of flow of 50 rad/sec at the link G. This source of flow generates a torque which rotates the link G and hence transmits motion to the rest of the links to actuate the entire mechanism. Fig. 6 indicates the variation of this generated torque with time which attains its maximum value initially and then becomes constant. This torque is required to start the motion of the system from its initial position of rest.

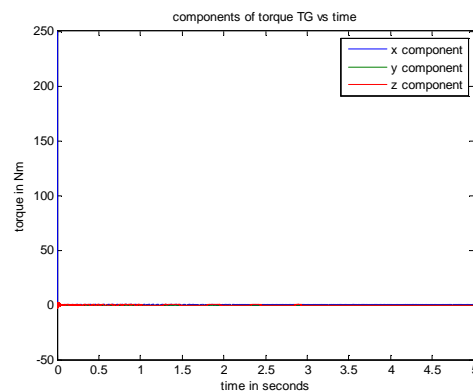


Fig. 6. Variation of torque with time

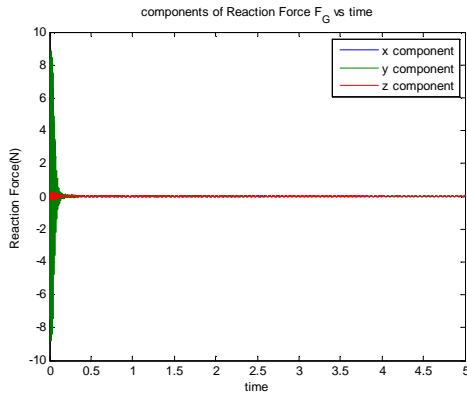


Fig. 7. Variation of reaction force with time

Fig. 7 shows the variation of components of reaction force on center of mass of link G w.r.t. time. Link G rotates in y-z plane about the x-axis as seen from the inertial frame. So, there is a component of reaction force in the y and z direction with decay in magnitude and becomes to zero as the link G gains its momentum.

### B. Link A (Crown Wheel or Arm)

Fig. 8 shows all the three columns of orientation matrix of the link A. The columns of the orientation matrix  ${}^0_A R$  represent the motion of tip of the unit vectors with respect to a stationary frame 0. Link A rotates in x-y plane about z axis as seen from the inertial frame. So, tip of the unit vector in x and y direction move in a circle and tip of the unit vector in z direction is a point because it does not change its orientation.

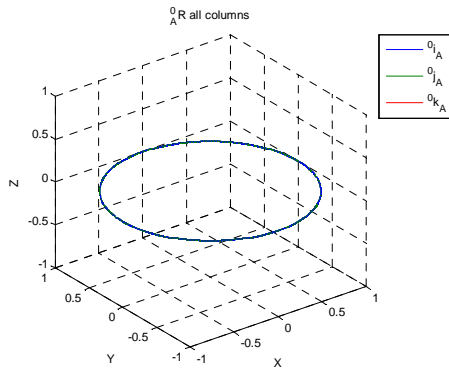


Fig. 8. Orientation matrix of link A,  ${}^0_A R$ .

Fig. 9 shows the variation of components of the position vector  ${}^0_{C_A} \vec{r}_{C_A}$  of the center of the mass of the link A with time which is constant because center of mass of link A does not change its position with the time. Hence, center of mass of link A does not trace any path.

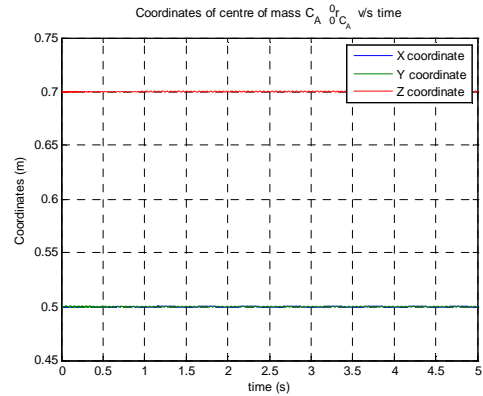


Fig. 9. Variation of coordinates of center of mass of link A with time

As indicated in fig. 10, the z component of angular momentum is constant with time because of constant source of flow imposed on the link G and because of link G and link A is in meshing and moving in opposite direction it is negative. The initial transients who arise due to the sudden imposition of source of flow  $S_f$  die down after a brief initial period due to damping.

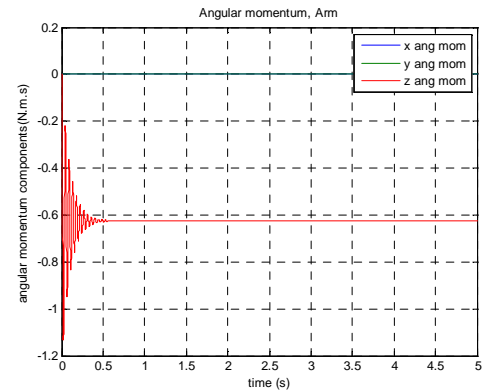
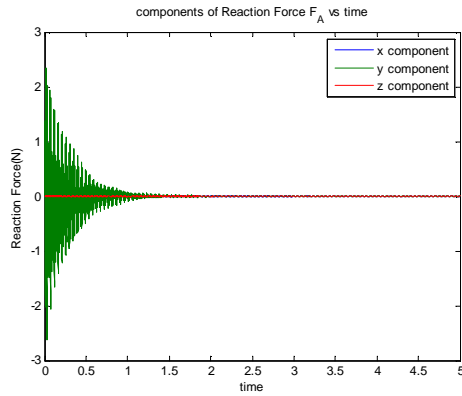
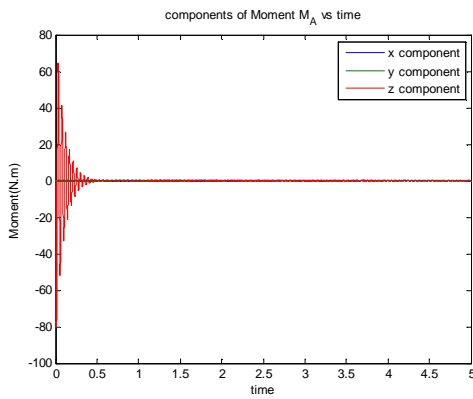


Fig. 10. Variation of components of momentum of link A with time.

Link A faces a periodic reaction force in x-direction and y-direction but with a retarding magnitude (approaches to zero) shown in fig. 11 (a). The cause behind the resulting curve is thrust force of rotating link G on link A. As the link A attains rotational inertia, this thrust changes into torque about z-axis. Similarly, in fig. 11 (b) initial moments in link A are observed because of stationary inertia of link A about z-axis, results in some stress development in the arm. With the link A gaining momentum, stresses die down and curve approaches to zero.



(a)



(b)

Fig. 11. Variation of components of reaction force and moment of link A with time

### C. Link S1 (Sun Gear 1)

Fig. 12 shows the orientation matrix of the link S1  ${}^0_{S1}R$ . In this case link S1 is fixed, so we do not get any projection of the tip of the unit vectors of the link S1 on frame 0.

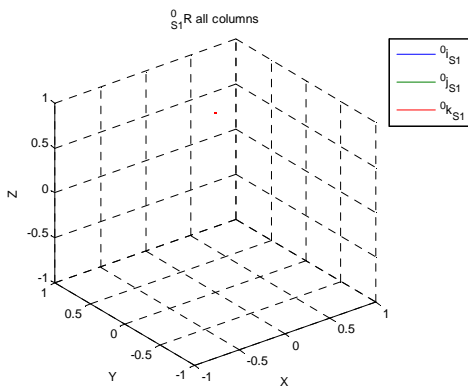


Fig. 12. Orientation matrix of link S1,  ${}^0_{S1}R$ .

Fig. 13 shows the variation of components of the position vector  ${}^0\overline{r}_{C_{S1}}$  of the center of the mass of the link S1 with time which is constant because center of mass of link S1 does not change its position with the time.

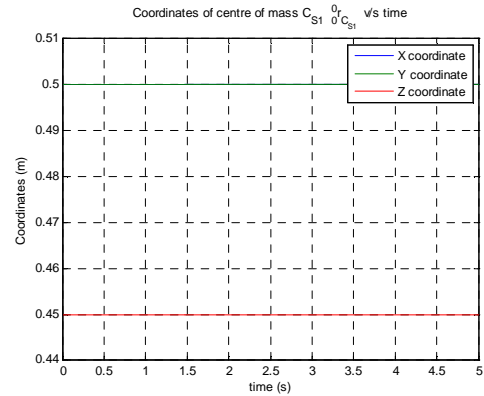


Fig. 13. Variation of coordinates of center of mass of link S1 with time

As link S1 is stationary so we do not get any component of angular momentum as shown in fig. 14 but because of source of flow imposed on link G, the initial transients are there which dies down gradually.

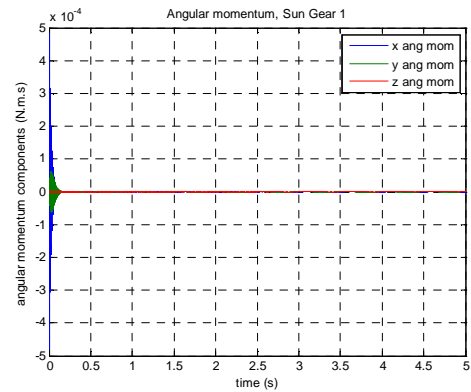


Fig. 14. Variation of components of momentum of link S1 with time

Fig. 15 shows the variation of components of reaction force on center of mass of link S1 w.r.t. time in x-direction and y-direction with retarding magnitude and approaches to zero because link S1 is fixed.

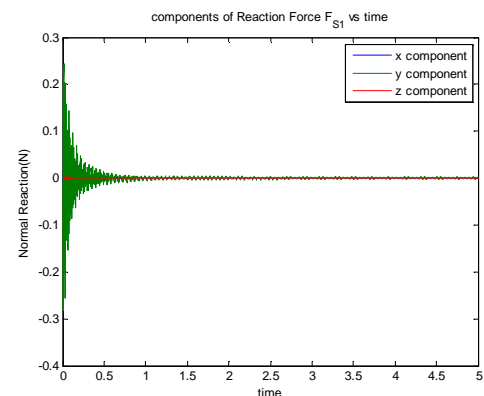


Fig. 15. Variation of components of reaction force of link S1 with time

#### D. Link S2 (Sun Gear 2)

Fig. 16 shows the complete orientation matrix of the link S2  ${}_{S_2}^0R$  in frame 0. The columns of the orientation matrix  ${}_{S_2}^0R$  represent the motion of tip of the unit vectors with respect to a stationary frame 0. Link S2 rotates in x-y plane about z axis as seen from the inertial frame. So, tip of the unit vector in x and y direction move in a circular path while the tip of the unit vector in z direction is a point because it does not change its orientation.

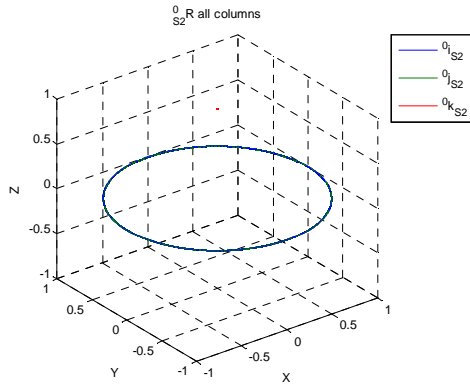


Fig. 16. Orientation matrix of link S2  ${}_{S_2}^0R$

Fig. 17 shows the variation of components of the position vector  ${}_{S_2}^0\vec{r}_{C_{S_2}}$  of the center of the mass of the link S2 with time which is constant because center of mass of link S2 does not change its position with the time.

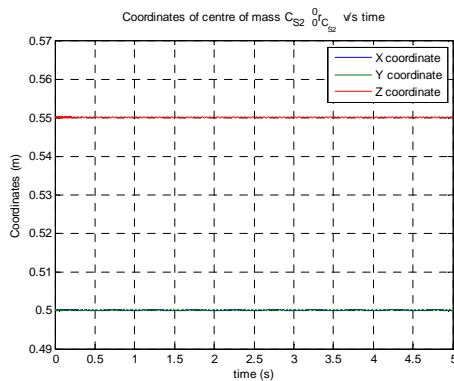


Fig. 17. Variation of coordinates of center of mass of link S2 with time

Fig. 18 shows the angular momentum of the components. Link S2 is rotating in x-y plane about the z-axis as seen from the inertial frame, so we get an angular momentum in z-direction which is constant because of constant source of flow imposed on link G.

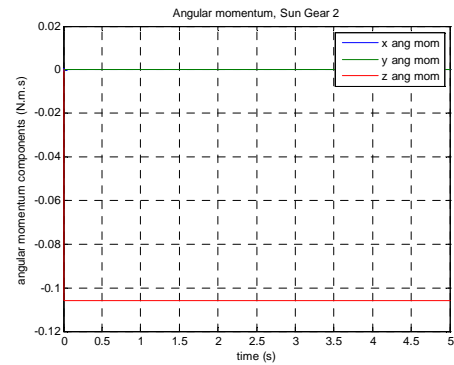


Fig. 18. Variation of components of momentum of link S2 with time

Fig. 19 shows the periodic variation of reaction force in x-direction and y-direction at center of mass of link S2 because of link S2 is rotating in x-y plane about z-axis as seen from the inertial frame. So, there is a component of reaction force in the x and y-direction with decay in magnitude and becomes to zero as the link S2 gains its momentum.

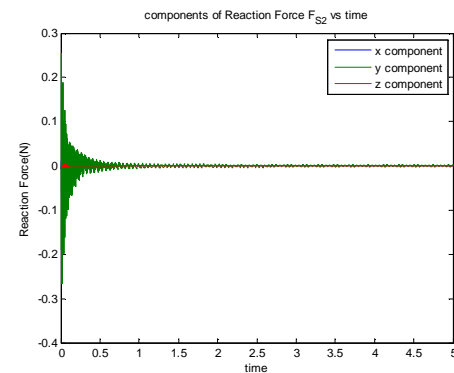


Fig. 19. Variation of components of reaction force of link S2 with time

#### E. Link P1 (Planet Gear 1)

Fig. 20 shows the motion of the tip of the unit vectors given by  ${}_{P_1}^0R$  indicating changing orientation of the link P1. The tip of unit vector in x and y direction having two motions or rotations i.e. one rotation about the axis of axle and second one is rotation about its own axis as seen from the inertial frame. And tip of the unit vector in z direction moves in a circular path as seen from the inertial frame.

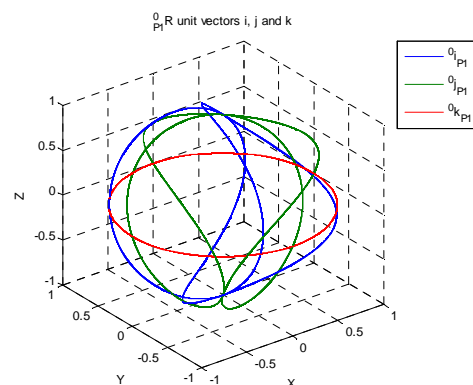


Fig. 20. Orientation matrix of link P1  ${}_{P_1}^0R$

The center of mass of the link P1 is rotating about the z-axis as seen from the inertial frame. Fig. 21 (a) indicates the variation of the components of the position vector of center of mass of the link P1. The z component is constant as the center of mass of the link P1 is rotating in the x-y plane about the z axis. The position of the x and y component of the center of mass are changing with time, so the route traced by center of mass of the link P1 is a circle, as shown in fig. 21 (b).

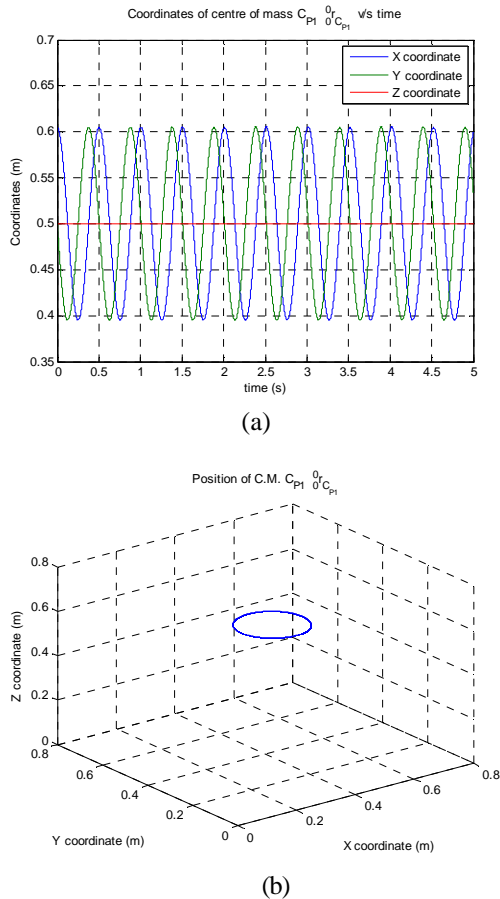


Fig. 21. Variation of coordinates of center of mass of link P1 with time

The variation of the translational momentum of the link P1 is indicated in fig. 22 (a). The x and y component of the translational momentum vector vary with time and the z component is 0, as the link P1 rotates about the z axis. Transients are observed at the beginning of the plot. These transients occur due to sudden imposition of the source of flow on the link G which dies down gradually due to damping. Fig. 22 (b) shows the angular momentum of the components. Link P1 is rotating about z axis so we get an angular momentum in z direction which is constant because of constant source of flow on link G. The x and y component of angular momentum is also there because of center of mass of link P1 is continuously changing.

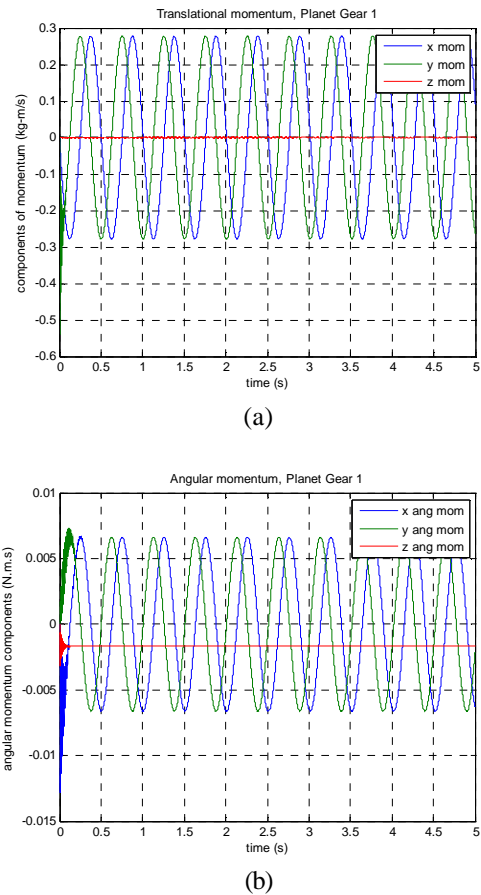
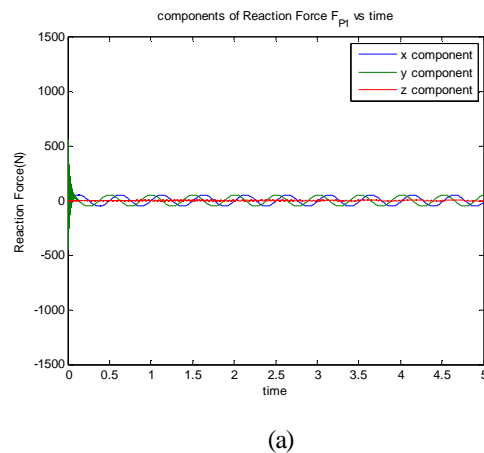


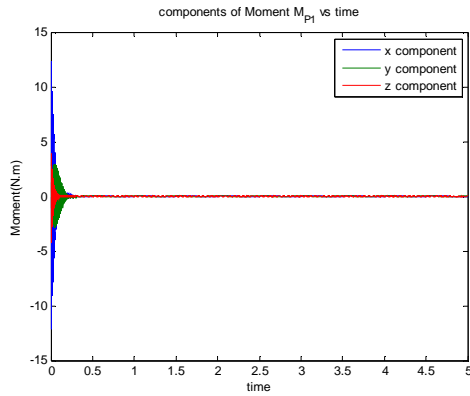
Fig. 22. Variation of components of momentum of link P1 with time

Fig. 23 (a) shows the x and y component of the reaction force vary with time and the z component is 0, as the center of mass of link P1 rotates about the z axis. Transients are observed at the beginning of the plot. These transients occur due to sudden imposition of the source of flow on the link G which dies down gradually due to damping. Fig. 23 (b) shows the component of moment in link P1. Initial transients are present in all the three directions because of, two motions of link P1.

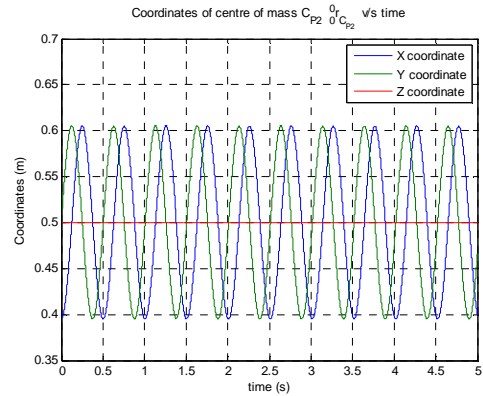


(a)





(b)



(a)

Fig. 23. Variation of reaction force and moment of link P1 with time

### F. Link P2 (Planet Gear 2)

Fig. 24 shows the motion of the tip of the unit vectors given by  ${}_{P2}^0R$  indicating changing orientation of the link P2. The tip of unit vector in x and y direction having two motions i.e. one rotation about the axis of axle and second one is rotation about its own axis as seen from the inertial frame. And tip of the unit vector in z direction moves in a circular path as seen from the inertial frame.

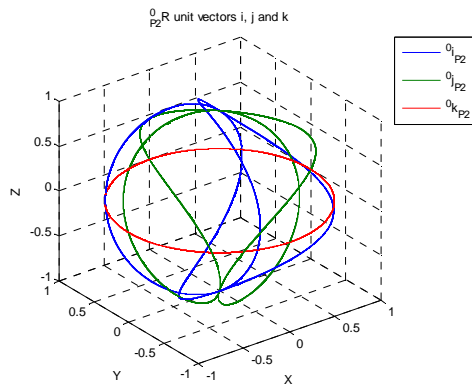
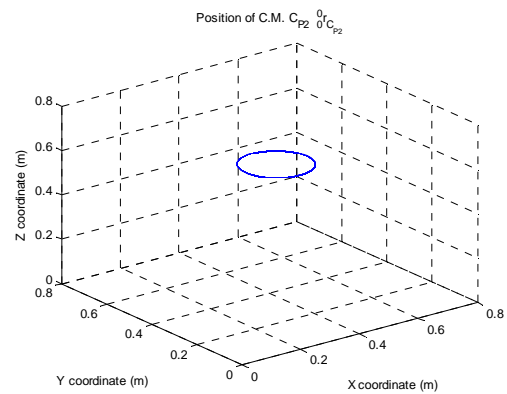


Fig. 24. Orientation matrix of link P2  ${}_{P2}^0R$

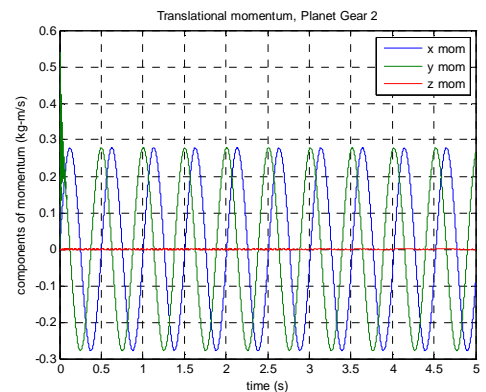
The center of mass of the link P2 is rotating about the z-axis as seen from the inertial frame. Fig. 25 (a) indicates the variation of the components of the position vector of center of mass of the link P2. The z component is constant as the center of mass of the link P2 is rotating in the x-y plane about the z axis. The position of the x and y component of the center of mass are changing with time, so the route traced by center of mass of the link P2 is a circle, as shown in fig. 25 (b).



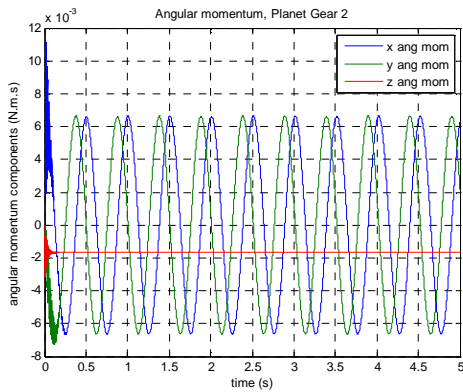
(b)

Fig. 25. Variation of coordinates of center of mass of link P2 with time

The variation of the translational momentum of the link P2 is indicated in fig. 26 (a). The x and y component of the translational momentum vector vary with time and the z component is 0, as the link P2 rotates about the z axis. Transients are observed at the beginning of the plot. These transients occur due to sudden imposition of the source of flow on the link G. As observed in the previous plots, the transients die down after some time and we observe a periodic variation of the translational momentum. Fig. 26 (b) shows the angular momentum of the components. Link P2 is rotating about z axis so we get an angular momentum in z direction which is a periodic type. Angular momentum in x and y direction is also there because of center of mass of link P2 is continuously changing.



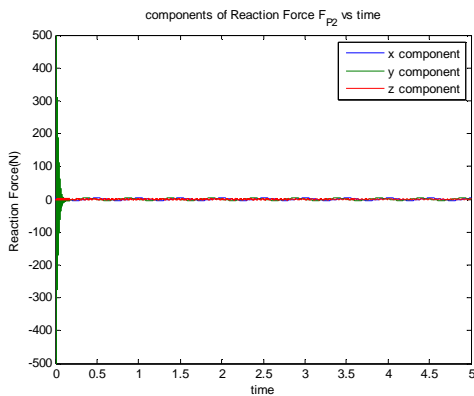
(a)



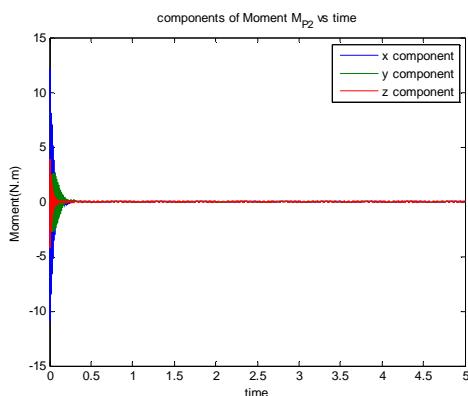
(b)

Fig. 26. Variation of components of momentum of link P2 with time

Fig. 27 (a) shows the x and y component of the reaction force vary with time and the z component is 0, as the center of mass of link P2 rotates about the z axis. Transients are observed at the beginning of the plot. These transients occur due to sudden imposition of the source of flow on the link G which dies down gradually due to damping. Fig. 27 (b) shows the component of moment in link P2. Initial transients are present in all the three directions because of, two motions of link P2.



(a)

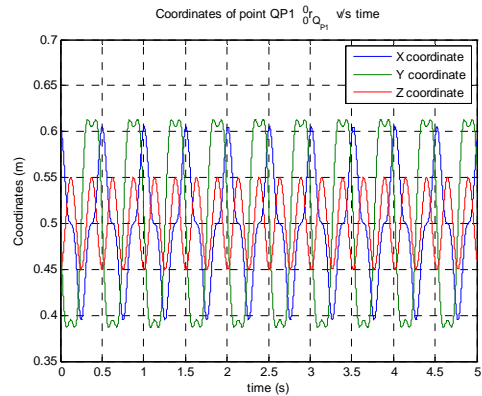


(b)

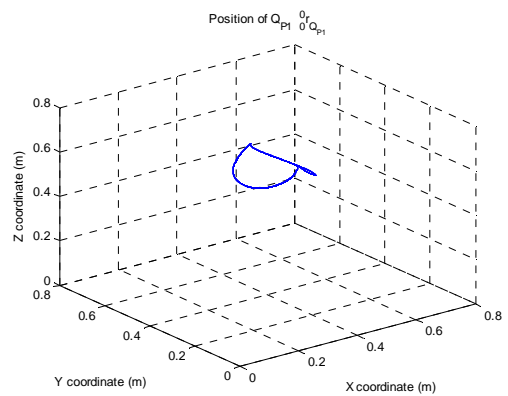
Fig. 27. Variation of reaction force and moment of link P2 with time

Fig. 28 (a) indicates the variation of coordinates of point  $Q_{P1}$  which is an arbitrary point on the link P1 (assuming extreme

point) which moves in all the three directions as seen from the inertial frame. So the position traced by the point  $Q_{P1}$  as it moves is shown in fig. 28 (b) which depends upon the gear ratio between the link P1 and link S1.



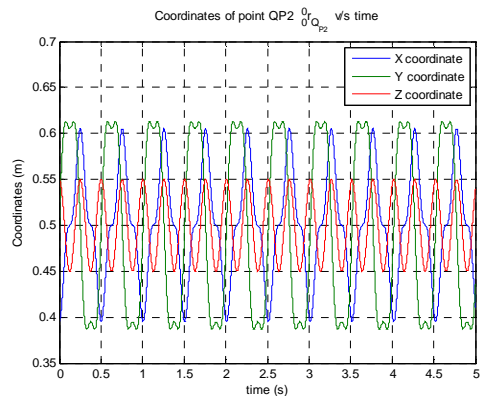
(a)



(b)

Fig. 28. Variation of coordinates of point  $Q_{P1}$  on link P1 with time

Fig. 29 (a) indicates the variation of coordinates of point  $Q_{P2}$  which is an arbitrary point on the link P2 (assuming extreme point) which moves in all the three directions as seen from the inertial frame. So the position drawn by the point  $Q_{P2}$  as it moves is shown in fig. 29 (b) which depends upon the gear ratio between the link P2 and link S2.



(a)

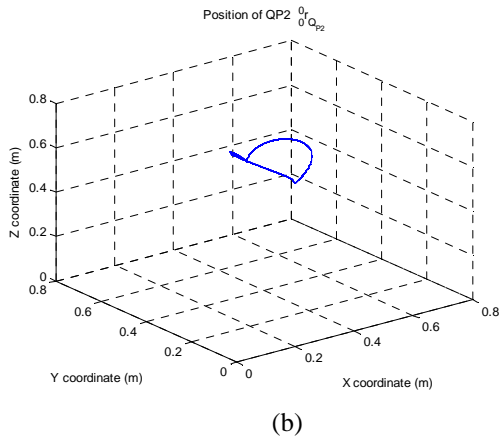


Fig. 29. Variation of coordinates of point  $Q_{P2}$  on link P2 with time

### G. Link H (Housing)

Fig. 30 shows the orientation matrix of the housing  ${}^0_H R$  express in frame 0. As discussed earlier, the link H is fixed because a source of flow  $S_F = \vec{0}$  acting on the 1-junction of the housing. So, we do not get any projection of unit vectors of frame H on frame 0.

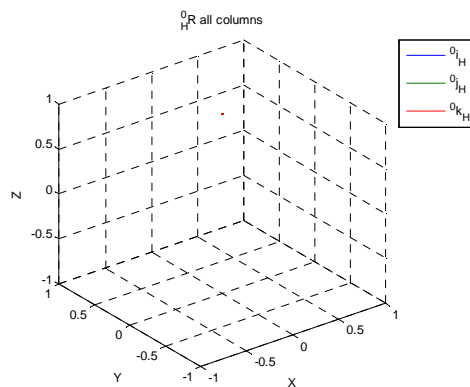


Fig. 30. Orientation matrix of link H  ${}^0_H R$

Link H is fixed and is at a constant distance from the inertial frame of reference in all the three directions as shown in fig. 31. So, we get a constant line as the time increases i.e.; 0.5 m.

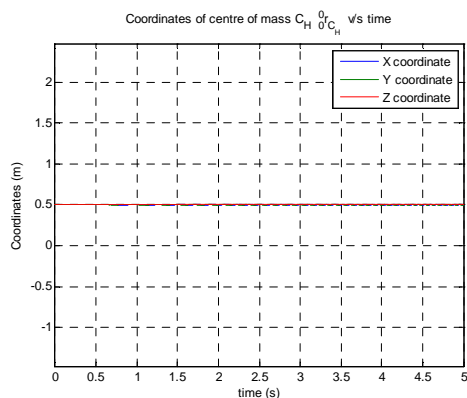


Fig. 31. Variation of coordinates of center of mass of link H with time

Fig. 32 shows the components of angular momentum of link H which is constantly reducing. This is due to the constant value of source of flow imposed on the link G from  $t = 0$ . After some time the components of momentum of the link H goes to zero or constant because link H is fixed.

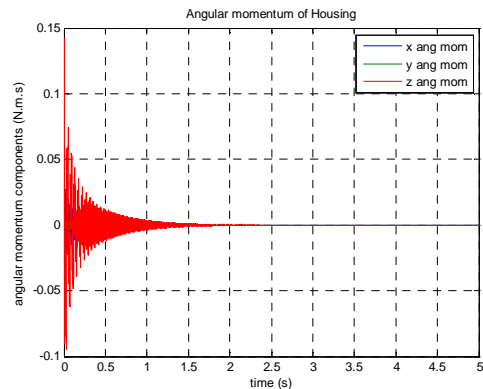
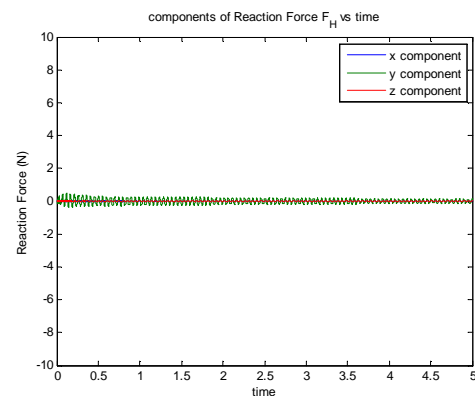
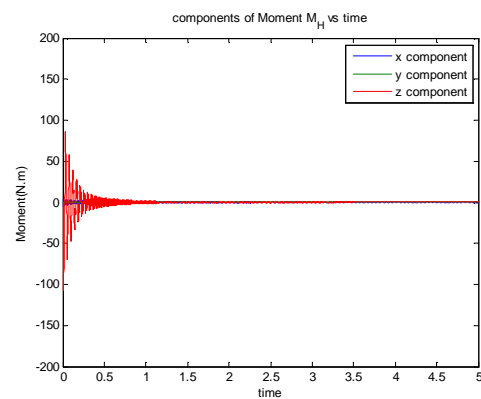


Fig. 32. Variation of components of momentum of link H with time

Fig. 33 (a) shows the components of the reaction force and fig. 33 (b) shows the component of moment of link H with time which is almost 0 because the link H is fixed. Transients are observed at the beginning of the plot. These transients occur due to sudden imposition of the source of flow on the link G, and decay due to damping.



(a)



(b)

Fig. 33. Variation of reaction force and moment of link H with time

## CONCLUSIONS

Dynamics of differential gear train mechanism has been modeled and simulated using the Bond Graph approach. Pictorial representation of the dynamics of translation and rotation for each link of the mechanism in the inertial frame, representation and handling of constraints at joints, and depiction of cause and effect relationships have been explained in this work. Code for simulation has been directly derived from the Bond Graph model.

Various simulation results have been obtained and discussed. These include columns of the orientation matrix of the links, position of center of mass of links with time, angular momentum of the links and position of any arbitrary point on each planet gear as it moves reaction forces and moments of the links at different locations, which are of interest from the design perspective. Transient dynamics arising due to sudden loading have also been effectively captured.

## REFERENCES

- [1] D. C. Karnopp, D. L. Margolis, and R.C. Rosenberg, System Dynamics: Modeling and Simulation of Mechatronic Systems, third edition, Wiley-interscience, 2000.
- [2] A. Mukherjee, R. Karmakar, Modeling and Simulation of Engineering Systems through Bondgraphs, Narosa Publishing House, New Delhi, 2000.
- [3] A. Ghosh and A. K. Mallik, Theory of Mechanisms and Machines, third edition, Affiliated East-West Press Private Limited, 1998.
- [4] S. S. Rattan, Theory of Machines, Second edition Tata McGraw Hill Publishing Company Limited, New Delhi, 2005.
- [5] <http://www.mathworks.com>
- [6] D. Karnopp, "An approach to Derivative Causality in Bond Graph Models of Mechanical Systems", J. Franklin Institute, vol. 329, No. 1, pp. 65-75, 1992.
- [7] A. Vaz, "Lecture notes: Bond Graph Modeling for Rigid Body Dynamics,". 2003. Unpublished.
- [8] M. J. L. Tiernego and A. M. Bos, "Modelling the Dynamics and Kinematics of Mechanical Systems with Multibond Graphs," Journal of The Franklin Institute, vol. 319, No. 1/2, pp. 37-50, 1985.
- [9] A. Vaz and S. Hirai, IMAACA 2004. Anand Vaz and Shinichi Hirai, "Modeling a Hand Prosthesis with Word Bond Graph Objects", Proceedings of The International Conference on Integrated Modeling & Analysis in Applied Control & Automation (IMAACA 2004), Oct. 28-31, 2004, Genoa, Italy, vol. 2, pp. 58-67.
- [10] Anand Vaz, "A Bond Graph Perspective of Computational Issues in Multibody Mechanics", Proceedings of NCMSTA'08, National Conference on Mechanism Science and Technology: from Theory to Application, Nov. 13-14, 2008, NIT Hamirpur, India, Keynote lecture, p. 842-853.
- [11] J. J. Craig, Introduction to Robotics: Mechanics and Control, third edition, Pearson Education Inc., 2005.